The Droplet Size Distribution in Cumulus Clouds in the 0.1 μm < r < 15 μm Range

Noah Wolfson

Department of Geophysics and Planetary Sciences, Tel Aviv University, Ramat Aviv, Tel Aviv, Israel

(Manuscript received 6 June 1978, in final form 29 December 1978)

ABSTRACT

Cloud droplet size distributions in the radius range from 0.1 to 15 μm have been investigated by remote sensing techniques. It was found that there is a large proportion of small droplets with radii <4 μm. The evolution of droplet size distribution in cold front clouds has been observed.

1. Introduction

Clouds are one of the most important agents controlling weather and climate. They are involved in the radiative transfer of energy and in the hydrological cycle and thus have to be treated in any model of the atmosphere, analytical or numerical. These studies, where parameterization is a necessity, often do not properly account for the cloud droplet size distribution (CDSD). This is partly due to the fact that the complete CDSD is not known. Our knowledge is especially poor in the range $r<4$ μm, where r is the radius of the droplet (Mason, 1971).

This range of sizes is of importance both for the cloud albedo to solar radiation fluxes and in cloud formation. In order to achieve better simulation and parameterization of the clouds in the various atmospheric models, an upgrading of our knowledge of the submicron droplets is essential (Mason, 1971).

2. Procedure

The CDSD will be retrieved here from data on the optical depth $\tau_{\text{ext}}(\lambda)$, as evaluated from measurements of the transmittance using a sun-following spectro-radiometer (Grassl, 1970) with a viewing angle of 0.25°. A full set of spectral measurements is attained once every 0.12 s. The optical depth is given by

$$\tau_{\text{ext}}(\lambda)=\int_{h_1}^{h_2}\int_0^\infty Q_{\text{ext}}\left(m_\lambda,\frac{2\pi r}{\lambda}\right)\pi r^2 n^1(r,h)\,dr\,dh, \quad (1)$$

where Q_{ext} is the Mie extinction coefficient, h_1 and h_2 are the cloud-base and cloud-top heights, respectively, λ is the wavelength, m_λ the refractive index of water, $n^1(r,h)$ the CDSD and h height in the cloud.

Q_{ext} is computed from Mie theory (Mie, 1908) with the assumption that the droplets are spherical. Multiple scattering is small for thin clouds and its contribution to τ in our spectro-radiometer with its small viewing angle is less than 2% (Grassl, 1970). Only thin clouds for which $\tau_{\text{ext}}(\lambda)<2$ will be investigated here. This limitation is due to the instrumental insensitivity for small signals. Since the geometrical depth of the cloud h_2-h_1 is not known it is convenient to define a columnar abundance

$$\int_{h_1}^{h_2} n^1(r,h)\,dh=\bar{n}(r)\Delta h=n(r_1,h_1,h_2), \quad (2)$$

where $\bar{n}(r)$ is the vertically averaged size distribution. On changing the order of integration of Eq. (1) and provided $r^2n(r_1,h_1,h_2)$ goes to zero at the integration limits, $\tau_{\text{ext}}(\lambda)$ can be expressed as

$$\tau_{\text{ext}}(\lambda)=\int_0^\infty Q_{\text{ext}}\left(m_\lambda,\frac{2\pi r}{\lambda}\right)\pi r^2 n(r_1,h_1,h_2)\,dr. \quad (3)$$

The integrand goes to zero at the integration limits and usually much before reaching the integration limits. [The integrand goes to zero as $r\rightarrow 0$ for at $r=0$ $n(r)$ and Q_{ext} equal zero and as $r\rightarrow\infty$, $n(r)\rightarrow 0$.] Therefore, it is possible to change the theoretical integration limits of Eq. (3) (Fymat, 1975) to appropriate finite and non-zero values:

$$\tau_{\text{ext}}(\lambda)\approx\int_a^b Q_{\text{ext}}\left(m_\lambda,\frac{2\pi r}{\lambda}\right)\pi r^2 n(r,h_1,h_2)\,dr. \quad (4)$$

The inaccuracy introduced by this approximation is dependent on the functional shape of $\pi r^2 n(r,h_1,h_2)$ which is unknown *a priori*.

The change in the limits of Eq. (3) enables one to convert the problem given in Eq. (4) into a discrete one. The spectro-radiometer described by Grassl (1970) performs simultaneous measurements of the direct solar radiation in up to eight wavelengths. The measure-

0022-4928/79/061053-08$06.00

ments were carried out continuously with and without clouds passing between the instrument and the sun. The optical depths were computed from the transmittances. As indicated previously, the measurement is taken at a very small viewing and scattering angle and therefore the effect of multiple scattering is minimized. The optical depths may be discretized in the following manner:

$$\left.\begin{array}{l}\tau_{\text{ext}}(\lambda_1) \approx \sum_{j=1}^{N} Q_{\text{ext}1,j}\pi r_j^2\bar{n}(r_j)\Delta r_j = \sum_{j=1}^{N} w_{1,j}\bar{n}(r_j) \\ \vdots \qquad\qquad\qquad \vdots \qquad\qquad\qquad \vdots \\ \tau_{\text{ext}}(\lambda_N) \approx \sum_{j=1}^{N} Q_{\text{ext}N,j}\pi r_j^2\bar{n}(r_j)\Delta r_j =) \sum_{j=1}^{N} w_{N,j}\bar{n}(r_j)\end{array}\right\} \tag{5}$$

or in matrix form

$$\boldsymbol{\tau} = W\bar{\boldsymbol{n}}, \tag{6}$$

where $\bar{n}(r_j)$ indicates an average over the corresponding interval Δr_j. Full explanation of these procedures are given by Fymat (1975). The Q_{ext}'s were computed as a function of r for each λ for which transmittance measurements were performed. The r_j's for Eq. (5) were chosen in such a way that for each λ they represent the radius, where $Q_{\text{ext}}(m_{\lambda_j}, 2\pi r/\lambda_j)$ reached its first maximum. The choice of the Δr's was made empirically according to

$$\left.\begin{array}{l}\Delta r_1 = r_2 - r_1 \\ \Delta r_j = (r_{j+1} - r_{j-1})/2 \\ \Delta r_N = r_N - r_{N-1}\end{array}\right\}.$$

The choice of the Δr_j's influences the values of the $w_{i,j}$ which in turn determine the stability of the derived solution (Twomey and Howell, 1967; Jackson 1972). Due to the change to finite limits a and b, the solution for the CDSD is nonunique and sometimes not even a continuous function of $\tau_{\text{ext}}(\lambda)$ (Fymat, 1975). Furthermore, the retrieved CDSD is not stable which means that small changes in $\bar{\tau}_{\text{ext}}(\lambda)$ may cause large variations in $\bar{n}(r)$.

The success of a numerical solution of Eq. (6) depends on the numerical structure of the matrix to be inverted. This is not necessarily W of Eq. (6)—the Twomey-Phillips (Phillips 1962; Twomey 1963) and Backus-Gilbert (Backus and Gilbert 1967, 1968, 1970) techniques use variants of W.

Tests were carried out for four inversion techniques and eight wavelengths (Wolfson *et al.*, 1978a). The accuracy of convergence to a known CDSD was evaluated by calculating the total error (ER). ER gives the absolute percentage deviation of the retrieved optical depths $\tau_i(\lambda)$ from those measured $\tau_m(\lambda)$ in all wavelengths:

$$\text{ER} = 100 \sum_{j=1}^{N} \frac{|\tau_i(\lambda_j) - \tau_m(\lambda_j)|}{\tau_m(\lambda_j)}. \tag{7}$$

3. Experimental results, analysis and conclusions

a. General description of the data analysis technique

Our experiment was in operation from October 1973 until April 1976. It was operated at full capability (eight wavelengths) from July 1974 onward. The wavelengths which were used were 0.4, 1.02, 1.26, 1.57, 2.20, 3.90, 9.30 and 11.00 μm. This spectral range determines the r_j's and Δr_j's in Eq. (5). The system is thus capable of supplying data on the CDSD in the $0.1\ \mu\text{m} < r < 15\ \mu\text{m}$ range. This range is adequate for the investigation of thin, low-based Cu and Sc clouds (Mason, 1971; Eldridge, 1957). These clouds, which were discrete, did not cover the sky completely and thus it was possible to measure the incident direct solar radiation with and without cloud interference. Cloud optical depths could thus be calculated directly.

During the period of measurements, raw data of discrete clouds from 21 days were chosen in the following manner. Only measurements from those days when one type of cloud was present and the sky background between the clouds was clear (without haze) were used. From each such day only some of the clouds, those accompanied by conditions of very stable sky radiation and short time of passage (<2 min) between the spectro-radiometer and the sun, were chosen for further study. (This selection process was necessary due to the failure of our analog-to-digital converter which forced manual evaluation of the raw data.) The spectral data chosen to be inverted from each individual cloud scan were all points with the local highest and lowest transmission in the clouds (peaks and lows of received radiation). Only data from those days with at least one cloud in which more than 50% of the points analyzed had an ER smaller than 10% were finally taken into account as it was found empirically that when ER was larger than 10% the retrieved CDSD's were generally unstable. Data from 33 clouds (Wolfson, 1977) collected on 13 days with 160 separate scan points were ultimately used.

b. Inversion procedure and application

The four inversion techniques which were previously investigated (Wolfson, 1978a,b) were applied to real data from some of the 33 clouds in order to decide upon an optimal method. It was found, as presented in Figs. 1–3, that there is not a significant difference in the retrieved CDSD's. The iterative Chahine method (Chahine, 1968) was chosen for use in our work for the following reasons:

1) It is especially suited to handling large volumes of data (Wolfson, *et al.*, 1978a,b).
2) It does not need any external tuning.
3) ER was found to be a monotonically decreasing function of the number of iterations.

The considerations elaborated on in the previous section led us to the following tactics. The inversion procedure was performed in steps. The first step was to perform the inversion with data from all channels. If ER was found to be larger than 10%, the noisiest channel (i.e., the channel with the largest contribution to ER) was eliminated and the inversion process was performed again. These eliminations resulted in decreasing ER which is our only criterion for convergence. This procedure was continued until ER was smaller than 10%. The number of channels used was never less than five. The channels usually left were 0.4, 1.02, 1.57, 3.9 and 9.3 μm which implies that the r_j's are 0.42, 1.07, 1.62, 3.7 and 11.25 μm, respectively.

c. General features of the CDSD in the 0.1 μm<r<15 μm range

The retrieved CDSD show, for the first time, the relative structure of the spectrum of cloud droplet sizes in the range 0.1 μm$<r<$4 μm. Typical examples are presented in Figs. 4–8. As the cloud depth h_2-h_1 is not known, the CDSD's are actually columnar abundances (cm^{-2} μm^{-1}). CDSD's in the figures can thus be compared with airborne measurements (e.g., Warner, 1969) only in a relative sense. It is evident that airborne measurements could have accurately determined the validity of the remotely sensed data for $r>4$ μm; however, there is no independent method to cross-check these results in the $r<4$ μm region.

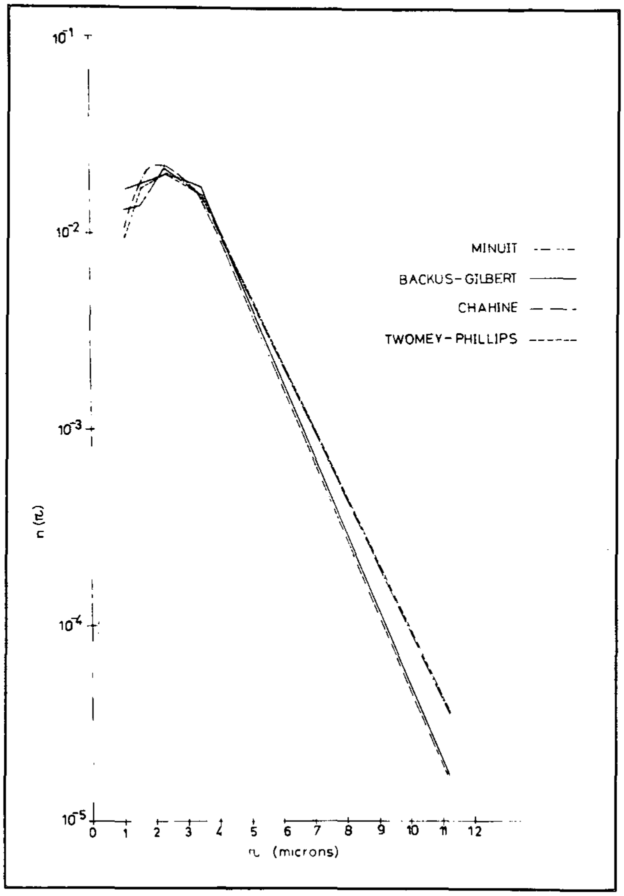

FIG. 1. Comparison of size distributions retrieved from one set of measurements from cloud 3 on 4 April 1976 as computed by four inversion techniques (The labels for the different inversion techniques are given in the upper right-hand corner.) Values of $n(r)$ are in units of cm^{-2} μm^{-1}.

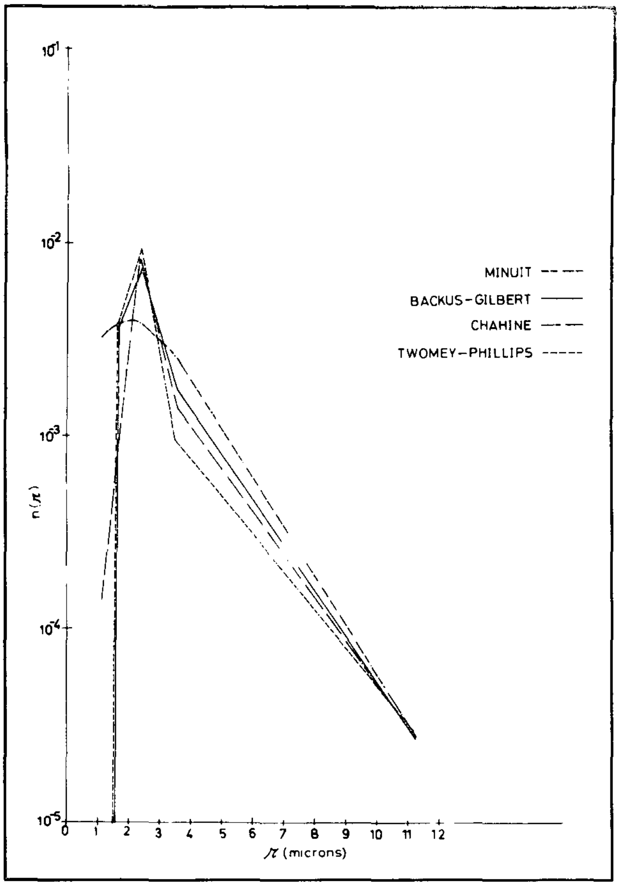

FIG. 2. As in Fig. 1 except for another set of data from cloud 3.

The results indicate a high percentage of small droplets. Their relative number is much larger than the relative number presently given in the literature (Weickmann and aufm Kampe, 1953; Warner 1969; Mason, 1971) for airborne measurements. The theoretical models for the CDSD in different cloud types given by Carrier *et al.* (1967) assume that $n(r)$ approaches zero as $r\rightarrow 0$ very rapidly. Our results do not show this and imply that this decrease is probably not as fast as given by Carrier.

In order to learn about the characteristics of the cloud microstructure without the need to compare many figures the following average quantities were

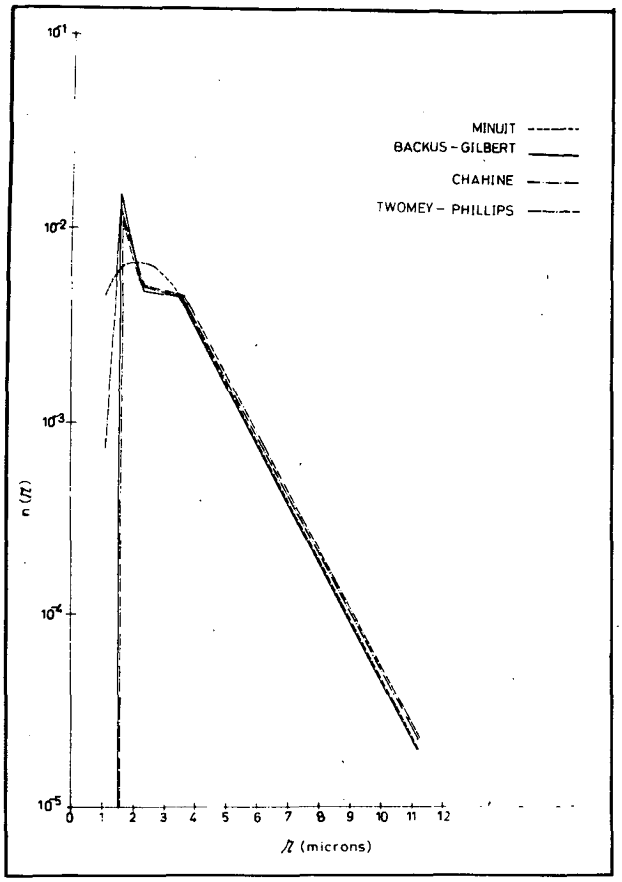

FIG. 3. As in Fig. 1 except for another set of data from cloud 3.

computed for each day:

1) The mean radius (R_{mean})

$$R_{\mathrm{mean}}=\frac{\sum_{j=1}^{N} n(r_j)\Delta r_j}{\sum_{j=1}^{N}\Delta r_j}.$$

2) The effective radius for scattering (R_{eff})

$$R_{\mathrm{eff}}=\frac{\sum_{j=1}^{N}\pi r_j^3 n(r_j)\Delta r_j}{\sum_{j=1}^{N}\pi r_j^2 n(r_j)\Delta r_j}.$$

3) The radius variance (R_{var})

$$R_{\mathrm{var}}=\frac{\sum_{j=1}^{N}(R_{\mathrm{eff}}-r_j)^2\pi r_j^2 n(r_j)\Delta r_j}{R_{\mathrm{eff}}^2\sum_{j=1}^{N} n(r_j)\pi r_j^2\Delta r_j}.$$

4) The dispersion (Dis),

$$\mathrm{Dis}=R_{\mathrm{var}}/R_{\mathrm{eff}}.$$

5) The percentage of the number of droplets in the two intervals with the smallest r_j's (Rat)

$$\mathrm{Rat}=\frac{100\sum_{j=1}^{2} n(r_j)\Delta r_j}{\sum_{j=1}^{N} n(r_j)\Delta r_j}.$$

6) The percentage of the volume of the droplets in the two intervals with the smallest r_j's (Vol)

$$\mathrm{Vol}=\frac{100\sum_{j=1}^{2} n(r_j)r_j^3\Delta r_j}{\sum_{j=1}^{N} n(r_j)r_j^3\Delta r_j}.$$

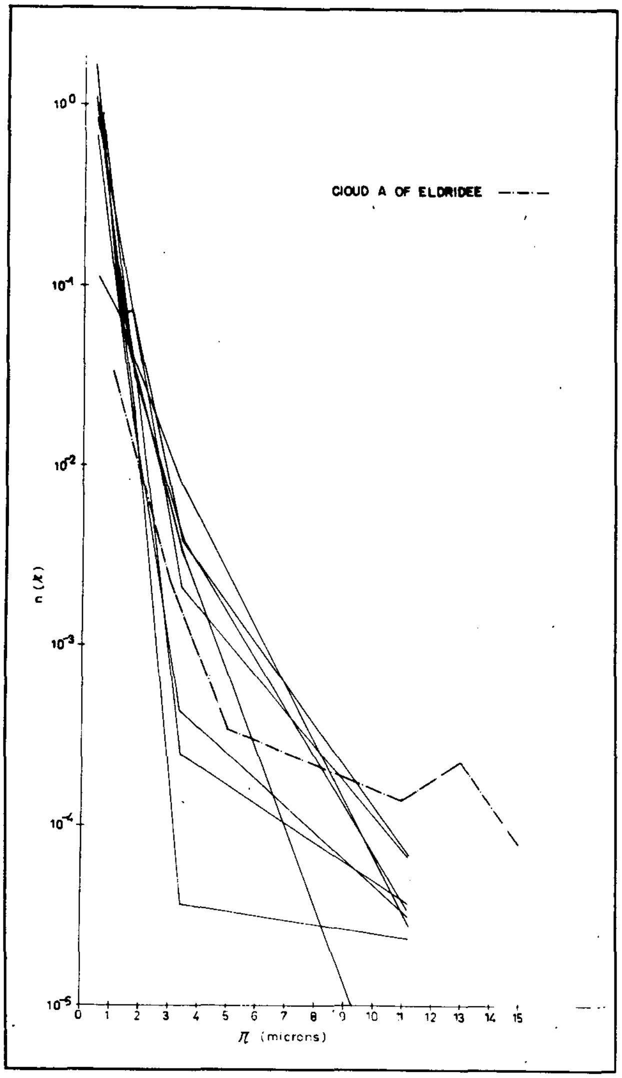

FIG. 4. CDSD's from 14 July 1975 cloud 3 [cloud A of Eldridge (1957) is also presented for comparison].

The results are presented in Tables 1 and 2.

The retrieved CDSD's usually display an exponential decrease between $r=1$ and $r=15$ μm. It was therefore found convenient to approximate them by a Junge-type distribution, $n(r)=cr^{-\nu}$ (values of c and ν are also given in Table 1). The exponent ν was found to average 2.7. The similarity in shape between the CDSD's and the average continental aerosol size distribution $n(r)=cr^{-3}$ (Junge, 1963) probably indicates the influence of the latter on the CDSD. This is due to the fact that the cloud droplets form on condensation nuclei; the cloud droplets are activated (by supersaturation) aerosols. Fitzgerald (1974) gives a theoretical discussion of the evolution of the cloud condensation nuclei spectrum to the unactivated haze and activated cloud droplet spectrum. Thus, one might suspect that our distributions contain both aerosols and cloud droplets. However, the optical depths from which we derive $n(r)$ are determined by the excess of attenuators in the cloud versus those outside. (This is due to the fact that in each case the background radiations before and after the cloud passage between the spectro-radiometer and the sun were identical.) Thus the atmospheric aerosol

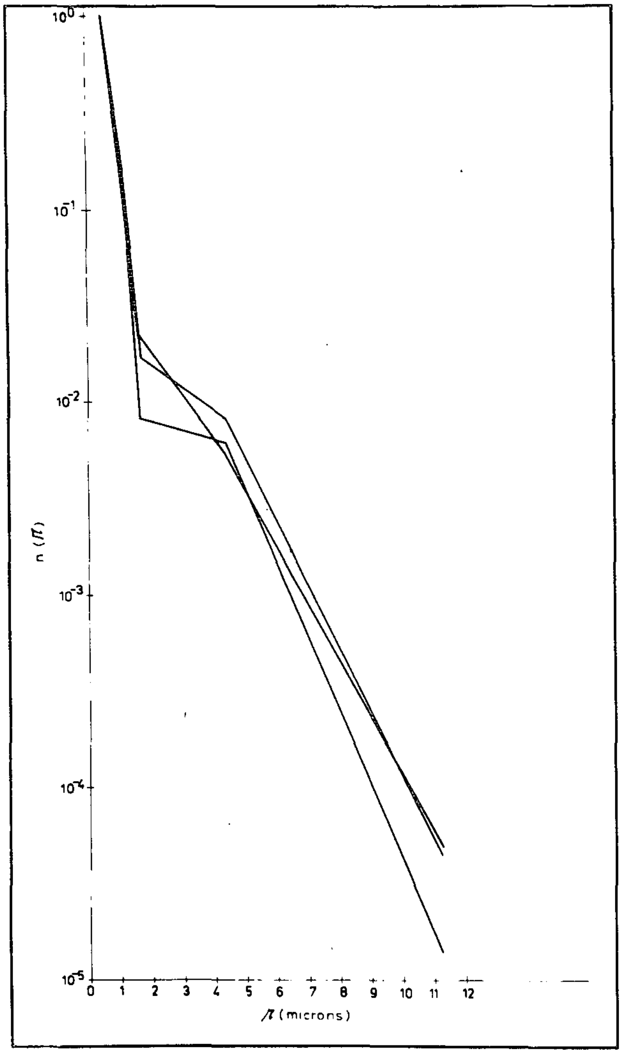

FIG. 5. As in Fig. 4 except for cloud 1.

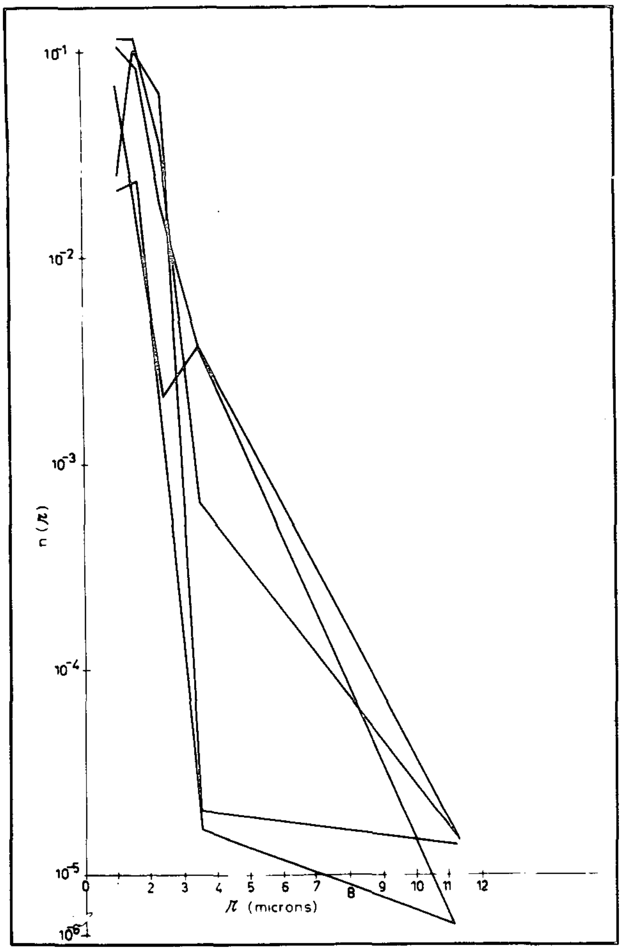

FIG. 6. CDSD's from 4 April 1976 cloud 1.

TABLE 1. Averaged typical parameters for water clouds.

log$c$	ν	Vol	Rat	Dis	R_{eff} (μm)	R_{mean} (μm)	Date (day-month-year)
−6.34	2.31	5.0	58.4	0.16	4.05	1.75	26/ 8/74
−9.85	0.76	2.6	39.4	0.15	4.34	2.04	20/ 9/74
−4.20	2.34	3.6	77.8	0.19	4.26	1.00	22/11/74
−5.21	2.82	9.8	98.7	0.39	3.95	0.52	5/ 1/75
−4.45	2.55	5.1	94.4	0.14	5.60	0.70	9/ 3/76
−3.11	3.29	14.0	91.1	0.34	1.69	0.54	30/ 5/75
−3.09	3.99	18.5	92.5	0.52	2.08	0.58	1/ 6/75
−2.75	3.10	10.7	88.8	0.54	2.20	0.55	12/ 6/75
−2.81	2.90	8.9	93.2	0.38	3.66	0.65	14/ 7/75
−3.42	2.62	21.5	94.5	0.24	1.84	0.60	17/ 7/75
−3.09	2.83	12.9	91.7	0.39	2.96	0.81	7/10/75
−3.86	3.23	14.4	95.2	0.45	3.15	0.67	9/10/75
−2.83	2.61	8.4	59.1	0.14	4.93	2.03	4/ 4/76
−4.23	2.72	10.4	82.7	0.31	3.44	0.96	Average values

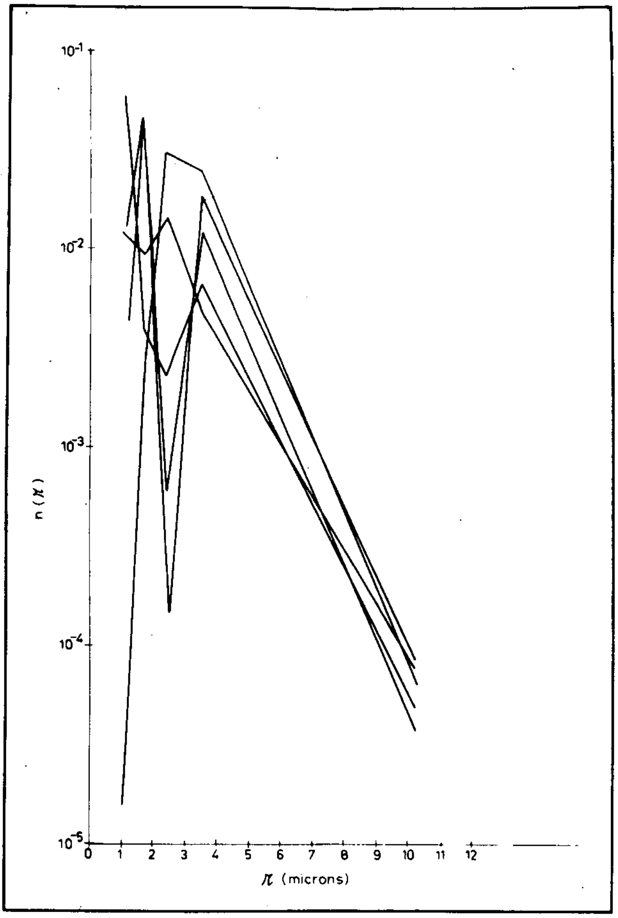

FIG. 7. As in Fig. 6 except cloud 2.

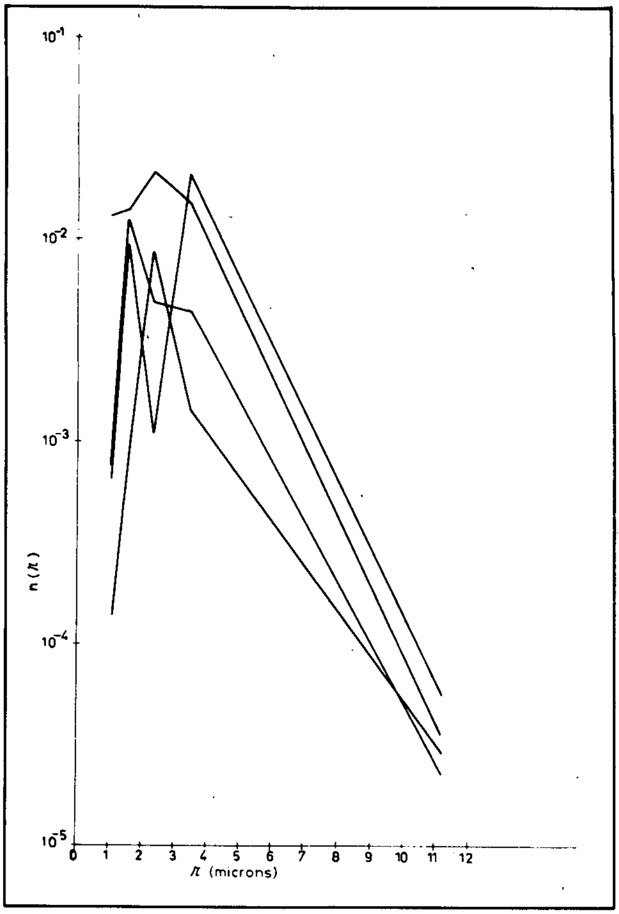

FIG. 8. As in Fig. 6 except for cloud 3.

concentrations for the column of air with and without the thin cloud are the same. Therefore, it is not probable that the small particles found in the submicron ranges are aerosols outside the cloud; the measured submicron particles are present only in the cloud.

The large number of the small droplets found clearly emphasizes the need to know more about the CDSD's in this size range in order to treat appropriately the radiative transfer of energy through clouds in the spectral domain of solar radiation. The cloud albedo to solar radiation is primarily determined by this size range.

There might be some agreements and also some differences between these results and theoretical models like those of Mason and Chien (1962), Árnason and Greenfield (1972), Warner (1973) and many others. These differences might be due to the following reasons:

1) The CDSD depends on the size spectrum of the activated aerosols. Spectra assumed in theoretical

TABLE 2. Daily weighted correlations between typical microphysical parameters (τ_{sh} is the optical depth of the cloud measured for the shortest wavelength).

	R_{mean}	R_{eff}	R_{var}	Dis	Rat	Vol	τ_{sh}	$-\nu$	log$c$
R_{mean}	1.00	0.49	−0.53	−0.51	−0.71	−0.41	0.47	0.47	−0.05
R_{eff}		1.00	−0.52	−0.76	−0.42	−0.68	0.26	0.48	−0.09
R_{var}			1.00	0.91	0.34	0.55	−0.51	−0.44	−0.11
Dis				1.00	0.47	0.64	−0.43	−0.30	−0.10
Rat					1.00	0.68	−0.45	−0.30	−0.10
Vol						1.00	−0.42	−0.36	−0.14
τ_{sh}							1.00	0.44	0.47
$-\nu$								1.00	0.04
log$c$									1.00

models are not necessarily similar to those (unknown) which were present in the formation of our clouds.

2) The evolution of the spectra is a composite of interactive processes which are each dependent on several atmospheric characteristics. Very little is known about the droplet size spectra in the range $r<4$ μm. Thus the models have to use many simplifying and sometimes unrealistic assumptions.

3) Some, but by no means the major part, of the differences between our results and the theoretical models may also be attributed to various inaccuracies of our methods. The error in the $\tau(\lambda)$ are of the order of 1 and 2%. The resulting effect of such an error in the accuracy of the retrieved CDSD's is extensively discussed in Wolfson *et al.* (1978a,b).

d. Synotic properties of the CDSD

The possibility of parameterizing the microphysical parameters of the cloud by the synoptic parameters of the free atmosphere was analyzed. The correlations between the atmospheric parameters as measured by a radiosonde and the retrieved average microphysical parameters were determined. The radiosonde measurements were performed at Bet-Dagan (10 km south east of Tel Aviv) by the Israel Meteorological Service. The pressure levels from which data was taken were 1000, 850, 700 and 500 mb. The use of these pressure levels is due to the fact that data only from such levels (standard levels) are used as an input for numerical forecasting models and thus available routinely now and in the future from radiosonde measurements. The correlations above 0.70 are presented in Table 3. The correlations are between R_{mean}, R_{eff}, Dis, Rat and Vol, and V_i, the southern component of the wind at level i, RH_i, the relative humidity at level i, $\mathrm{DF}|_j^i$, the wind shear between levels i and j, $dT/dz|_j^i$ the temperature lapse rate between levels i and j, and $d\theta/dz|_j^i$, the potential temperature gradient between levels i and j.

The correlations are rather poor and indicate that the parameterization of the CDSD by radiosonde data is, to say the least, very difficult. As the correlations are low, no effort is made to present any physical reasoning for them. The failure of the radiosonde to offer an explanation to the characteristics of the CDSD might be due to the facts that the radiosonde does not measure all the parameters which influence the growth of the CDSD and the radiosonde gives data on a synoptic scale, while a cloud is a much more local phenomena.

TABLE 3. Linear correlations between meteorological parameters and microphysical parameters of water clouds (only correlations above 0.70 are presented).

Synoptic parameters	Cloud microphysical parameters R_{mean}	R_{eff}	Dis	Rat	Vol
$V_{700\ \mathrm{mb}}$	0.76	0.70	−0.71	−0.74	−0.70
$\mathrm{RH}_{1000\ \mathrm{mb}}$	−0.70			0.78	
$\mathrm{DF}\big\|_{700\ \mathrm{mb}}^{850\ \mathrm{mb}}$	0.70	0.75			
$dT/dz\big\|_{700\ \mathrm{mb}}^{1000\ \mathrm{mb}}$		−0.78			
$\theta_{700\ \mathrm{mb}}$		−0.73			
$d\theta/dz\big\|_{700\ \mathrm{mb}}^{1000\ \mathrm{mb}}$		−0.78	0.74		

e. The CDSD of cold front and typical summer clouds

Many sequences of measurements were analyzed during the course of our investigation. We shall focus our attention here on two typical sets. The first one from 14 July 1975 was a typical summer day. The second on 4 April 1976, was taken during the passage of a cold front during which measurements were carried out until the onset of rain. These two sets, presented in Figs. 4–8, enable us to try and demonstrate some general conclusions as to the process of CDSD evolution.

There seem to be three stages which are experimentally discernible.

- The initiation of a Junge-type CDSD. This spectrum which is presented in Figs. 4 and 5 for 14 July 1975, a typical summer day, is formed by condensation of water on activated aerosols. Some clouds show this type of CDSD throughout their life cycle (Junge-type CDSD's have been measured for all parts of the clouds).
- The spectra of the droplet sizes develops a second maximum in addition to the one present in the small radius range. Such CDSD's are presented in Figs. 6 and 7 and were acquired on 4 April 1976 during the passage of a cold front. Such a spectrum is formed when the droplets grow by condensation while there is also a continuing activation of new droplets due to condensation.
- Size spectra develop with a maximum in the range $r>2$ μm (see Fig. 8). This spectrum is narrower than those at the first two stages and it indicates further development of the CDSD as the rain stage of the cloud life cycle is approached.

These three observed stages are similar to those presented in the theoretical studies by Arnason and Greenfield (1972). Although the three stages have not been observed in one cloud life cycle, the sequence outlined here is a plausible interpretation of the different general types of CDSD's which have been retrieved.

4. Summary

The present study enables one for the first time to analyze a large sample of CDSD's in the hitherto unsampled range of 0.1 μm$<r<$4 μm and to deduce some preliminary conclusions as to their properties. The present contributions are relevant to the study of radiative transfer of solar energy through clouds as well as to cloud microphysics. It should be remembered, however, that these remotely sensed CDSD's have not been validated by any simultaneous airborne measurements.

Acknowledgment. This research is part of a dissertation submitted to Tel Aviv University in partial fulfillment of the requirements for a Ph.D. degree. I should like to thank Prof. J. H. Joseph and Dr. Y. Mekler for many fruitful discussions. This research was partly financed by the Deutsche Forchungsgemeinschaft through contracts BO 197/9 and 197/18 which were mediated through Prof. H. J. Bolle of the University of Munich (F.R.G.). I am also grateful for the excellent support from John Pinnons who was responsible for the installation and the technical maintenance of the laboratory.

REFERENCES

Árnason, G., and R. S. Greenfield, 1972: Micro- and macrostructures of numerically simulated convective clouds. *J. Atmos. Sci.*, **29**, 342–367.

Backus, G. E., and J. F. Gilbert, 1967: Numerical application of a formalism for geophysical inverse problems. *Geophys. J. Roy. Astron. Soc.*, **13**, 247–276.

——, and ——, 1968: The resolving power of gross earth data. *Geophys. J. Roy. Astron. Soc.*, 16, 169–205.

——, and ——, 1970: Uniqueness in the inversion of inaccurate gross earth data. *Phil. Trans. Roy. Soc. London*, **A226**, 123–192.

Carrier, L. W., G. A. Cato and K. J. von Essen, 1967: The backscattering and extinction of visible and infrared radiation by selected major cloud models. *Appl. Opt.*, **6**, 1209–1216.

Chahine, M. T., 1968: Determination of temperature profile in the atmosphere from the outgoing radiance. *J. Opt. Soc. Amer.*, **58**, 1634–1637.

Eldridge, R. E., 1957: Measurements of cloud droplet size distributions. *J. Meteor.*, **14**, 55–59.

Fitzgerald, J. W., 1974: Effect of aerosol composition on cloud droplet size distribution, a numerical study. *J. Atmos. Sci.*, **31**, 1358–1367.

Fymat, A. L., 1975: Remote monitoring of environmental particulates pollution—A problem in inversion of first kind integral equations. *Appl. Math. Comput.*, 1, 131–185.

Grassl, H., 1970: Determination of cloud droplet size distribution from spectral transmission measurements. *Beit. Phys. Atmos.*, **43**, 255–284.

Hansen, J. E., and L. D. Travis, 1974: Light scattering in planetary atmospheres. *Space Sci. Rev.*, **1**, 527–610.

Jackson, D. D., 1972: Interpretation of inaccurate, insufficient and inconsistent data. *Geophys. J. Roy. Astron. Soc.*, **28**, 97–109.

Junge, C., 1963: *Air Chemistry and Radioactivity.* Academic Press, 382 pp.

Mason, B. J., 1971: *The Physics of Clouds*, 2nd ed. Clarendon Press, 659 pp.

——, R. Emig, 1961: Calculation of the ascent of a saturated buoyant parcel with mixing. *Quart. J. Roy. Meteor. Soc.*, **87**, 212–222.

——, C. W. Chien, 1962: Cloud droplet growth by condensation in cumulus. *Quart. J. Roy. Meteor. Soc.*, **88**, 136–142.

Mie, G., 1908: Beitrag zur optik trueber medien. *Ann. Phys.*, **25**, 377–445.

Phillips, D. L., 1962: A technique for the numerical solution of certain integral equations of the first kind. *J. Assoc. Comput. Mach.*, **9**, 84–97.

Twomey, S., 1963: On the numerical solution of Fredholm equations of the linear system produced by a quadrature. *J. Assoc. Comput. Mach.*, **10**, 97–101.

——, and H. B. Howell, 1967: Some aspects of the optical estimation of microstructure in fog and cloud. *Appl. Opt.*, **6**, 2125–2131.

Warner, J., 1969: The microstructure of cumulus cloud. Part I. General features of the droplet spectrum. *J. Atmos. Sci.*, **26**, 1049–1059.

——, 1973: The microstructure of cumulus cloud. Part IV. The effect on the droplet spectrum of mixing between cloud and environment. *J. Atmos. Sci.*, **30**, 256–261.

Weickmann, H. K., and H. J. aufm Kampe, 1953: Physical properties of cumulus clouds. *J. Meteor.*, **10**, 204–211.

Wolfson, N., 1977: Investigation of the droplet size distribution in the range $0.1\ \mu m < r < 15\ \mu m$ in thin water clouds using solar spectral transmission measurements. Ph.D. dissertation, Tel Aviv University, 151 pp.

——, J. H. Joseph and Y. Mekler, 1978a: Comparative study of inversion techniques. Part I: Accuracy and stability. *J. Appl. Meteor.*, **18**, 543–555.

——, —— and ——, 1978: Comparative study of inversion techniques Part II: Resolving power, conservation of normalization and superposition principles. *J. Appl. Meteor.*, **18**, 556–561.